



# Determination of the Relative Configuration of Terminal and Spiroepoxides by Computational Methods. Advantages of the Inclusion of Unscaled Data

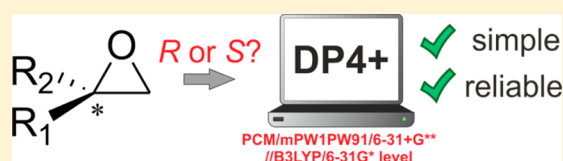
María M. Zanardi,<sup>†,‡</sup> Alejandra G. Suárez,<sup>†</sup> and Ariel M. Sarotti<sup>\*,†</sup>

<sup>†</sup>Instituto de Química Rosario (CONICET), Facultad de Ciencias Bioquímicas y Farmacéuticas, Universidad Nacional de Rosario, Suipacha 531, Rosario 2000, Argentina

<sup>‡</sup>Facultad de Química e Ingeniería del Rosario, Pontificia Universidad Católica Argentina, Av Pellegrini 3314, Rosario 2000, Argentina

## S Supporting Information

**ABSTRACT:** The assignment of the relative configuration of spiroepoxides or related quaternary carbon-containing oxiranes can be troublesome and difficult to achieve. The use of GIAO NMR shift calculations can provide helpful assistance in challenging cases of structural elucidation. In this regard, the DP4 probability is one of the most popular methods to be employed when only one set of experimental data is available, though modest results were obtained when dealing with spiroepoxides. Recently, we introduced an improved probability (DP4+) that includes the use of both scaled and unscaled NMR data computed at higher levels of theory. Here, we report a comprehensive study to explore the scope and limitations of the DP4+ methodology in the stereoassignment of terminal or spiroepoxides bearing a wide variety of molecular complexity and conformational freedom. The excellent levels of correct classification achieved were interpreted on the basis of a constructive compensation of errors upon using both scaled and unscaled proton and carbon data. The advantages of the DP4+ methodology in solving two case studies that could not be unequivocally assigned by NOE experiments are also provided.



## INTRODUCTION

Epoxides are among the most useful functional groups in organic chemistry. Apart from being present in many biologically active natural products, such as the mitomycins, azinomycins, and epothilones, they are extremely versatile building block in organic synthesis.<sup>1</sup> Its synthetic utility is due to the strain associated with the three-membered heterocycle, which is “spring-loaded” for reactions with nucleophiles, allowing a wide array of functionalization strategies to be achieved with high stereo- and regioselectivity. Therefore, the preparation of epoxides has been of considerable interest and many methods have been developed to date, including oxygen transfer to alkenes, intramolecular nucleophilic displacements, and additions to carbonyl compounds.<sup>1</sup>

The determination of the relative configuration of quaternary carbon-containing epoxides (such as the case of spiroepoxides) can be often troublesome and difficult to achieve by using only NMR data, as NOE measurements can lead to ambiguous results because of the  $sp^2$ -like character of the carbon atoms of the oxirane ring (vide infra).<sup>2</sup> The use of NMR anisotropic interactions, such as residual dipolar couplings (RDCs) and residual chemical shift anisotropy (RCSAs), represent useful strategies that could be used in these cases.<sup>3</sup> The relative configuration of complex organic molecules (including those bearing several quaternary carbon atoms) could be efficiently determined by these methods.<sup>3</sup> In this regard, the need of special media to perform the molecular alignment in anisotropic media represents one of the main limitations of

these methods, though impressive advances have been achieved in the field.<sup>3</sup> On the other hand, NMR calculations with quantum-based methods represents a simple and useful alternative to determine the relative configuration of epoxides, avoiding chemical derivatization (inappropriate when low amount of sample is available) or X-ray studies (unfeasible in several cases).<sup>4–6</sup> The structure and stereochemistry of a wide variety of complex natural products have been assigned or revised on the basis of NMR calculations with remarkable levels of confidence, emerging as indisputable new tools in NMR spectroscopy.<sup>4–6</sup> Several strategies have been developed to correlate the experimental and theoretically computed chemical shifts, including CP3,<sup>7</sup> DP4,<sup>8</sup> and ANN-PRA<sup>9</sup> (artificial neural network pattern recognition analysis).<sup>5a</sup> In this regard, the DP4 probability is the most accurate and popular method to determine the correct stereostructure of an organic molecule when only one set of experimental data is available (as in the case of isomerically pure compounds). This method was developed by the Goodman group in 2010 and was used in the structural assignment or revision of plenty natural and unnatural products,<sup>8</sup> many of them verified by total synthesis of the most likely structure.<sup>5a,10</sup> Recently, we introduced a modified probability (DP4+), demonstrating that the inclusion of unscaled data and the use of higher levels of theory for the GIAO NMR calculation procedure resulted in a significant

Received: August 29, 2016

Published: November 4, 2016



improvement in the classification performance of the method.<sup>11</sup> We showed that the original DP4 probability consistently afforded poor results when dealing with spiroepoxides (compounds 1–7, Figure 1), providing further evidence of

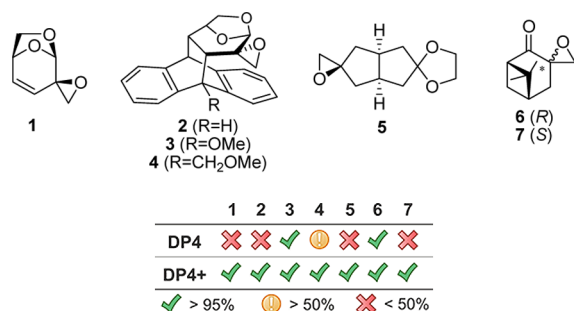


**Figure 1.** Seven examples of spiro epoxides used in the evaluation of the DP4+ probability.

the challenge involved in the stereoassignment of these types of compounds. In four cases (compounds 1, 2, 5, and 7), the incorrect isomer was identified in high probability (the worst scenario), whereas in one of the remaining examples (compound 4) the correct isomer was successfully assigned in modest confidence (50–95%). In contrast, our DP4+ probability succeeded in correctly pointing toward the correct isomer with high probability (>95%) in all cases.

The use of DP4+ in the stereoassignment of epoxides was also highlighted by a recent work of Tagliatela–Scafati and co-workers on the structural elucidation of plakdiepoxide, isolated from the Chinese sponge *Plakortis simplex*.<sup>12</sup>

Given the importance of alternative and reliable methods to provide assistance in the stereochemical assignment of spiro or related quaternary carbon-containing epoxides, we explored the scope and limitations of DP4+ as a benchmark methodology to be used whenever the NMR data are not conclusive.

## RESULTS AND DISCUSSION

To accomplish our goals, we selected 24 spiro- or terminal epoxides from the recent literature (compounds 8–31, Figure 2)

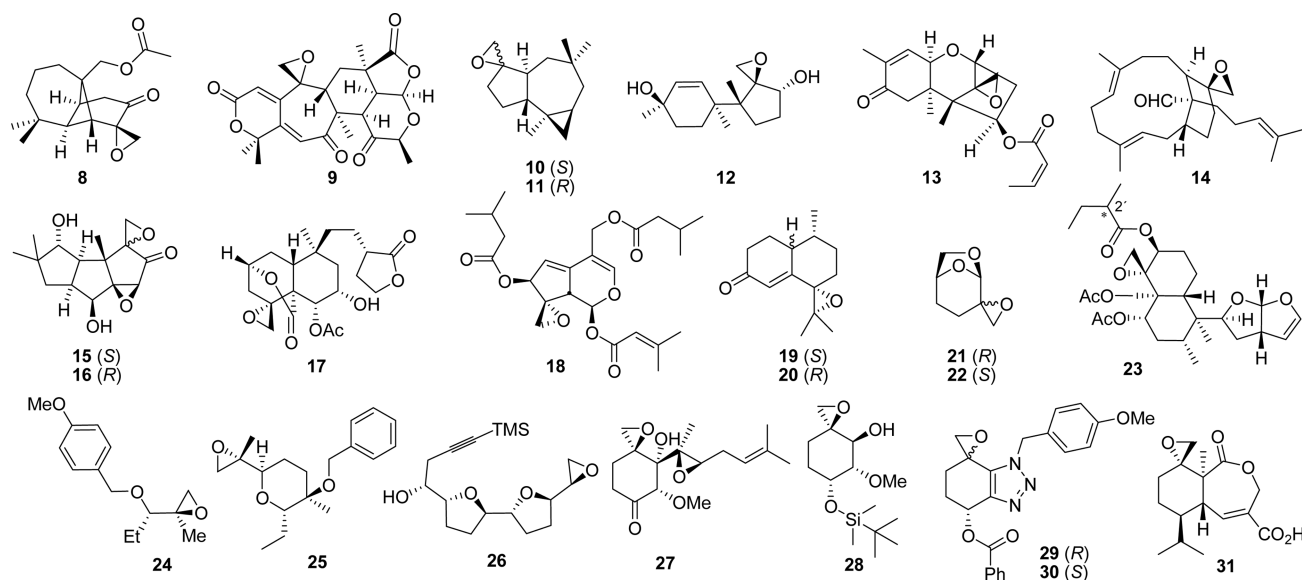


**Figure 2.** Twenty-four selected spiro or terminal epoxides used in this study.

2), including two unpublished examples from our own synthetic work (compounds 21 and 22, Figure 2), with known relative configuration (established by X-ray analysis, chemical synthesis, or irrefutable NMR data).<sup>13,14</sup> In addition, we foresaw a wide variety of molecular complexity, functional groups, and conformational freedom in the selected compounds. Following the DP4+ general procedure, the chemical shifts were computed at the PCM/mPW1PW91/6-31+G\*\*//B3LYP/6-31G\* level of theory using the GIAO method implemented in Gaussian 09.<sup>11</sup>

With the shielding tensors in hand, we evaluated the DP4+ performance in establishing the correct configuration at the epoxide stereocenter using the Excel spreadsheet provided free of charge at [sarotti-NMR.weebly.com](http://sarotti-NMR.weebly.com) or as part of the Supporting Information of the original reference.<sup>11</sup> Briefly, the DP4+ probability is a modified version of DP4 in which  $P(i)$  is the probability that candidate  $i$  (out of  $m$  isomers) is correct and is a function of the corresponding probabilities computed using scaled and unscaled chemical shifts, termed  $sDP4+$  and  $uDP4+$ , respectively. Moreover, each DP4+ term can be calculated using only  $^1H$  data,  $^{13}C$  data, or both.

In Figure 3, we show the result of the DP4+ probabilities computed for the 24 examples shown in Figure 2, along with the corresponding probabilities using only unscaled or scaled shifts ( $uDP4+$  and  $sDP4+$ , respectively), computed from  $^1H$  data,  $^{13}C$  data, or both. We also included the results obtained for the seven examples previously reported by us (compounds 1–7) to provide insightful discussion. Since no strictly defined cutoff limits are imposed, the probability computed for a given isomer indicates the level of certainty of the assignment itself. Thus, we have identified three different scenarios depending on the confidence level of the associated probability: the optimal (indicated in green) represents a correct assignment made in high probability (>95%), the acceptable (indicated in yellow) represents a correct assignment made in lower probability (50–95%), and the bad (indicated in red) represents cases in which the correct isomer is assigned with low probability (<50%).

At first glance, the results provided in Figure 3 indicate the excellent performance of the DP4+ probability in successfully assigning the right isomer in high certainty. Not only was none

N°	sDP4+			uDP4+			DP4+		
	H	C	all	H	C	all	H	C	all
1	✓	✓	✓	✗	✓	✓	✗	✓	✓
2	✓	✗	✓	✓	✓	✓	✓	✓	✓
3	✓	✓	✓	✓	✓	✓	✓	✗	✓
4	✓	✗	✓	✓	✓	✓	✓	✗	✓
5	✗	✓	✓	✓	✓	✓	✗	✓	✓
6	✓	✓	✓	✓	✓	✓	✓	✓	✓
7	✗	✓	✓	✗	✓	✓	✗	✓	✓
8	✗	✓	✓	✓	✓	✓	✗	✓	✓
9	✗	✓	✓	✓	✓	✓	✗	✓	✓
10	✗	✓	✓	✗	✓	✓	✗	✓	✓
11	✓	✓	✓	✓	✓	✓	✓	✓	✓
12	✓	✗	✓	✓	✗	✓	✓	✗	✓
13	✓	✗	✗	✓	✓	✓	✓	✗	✓
14	✓	✓	✓	✓	✓	✓	✓	✓	✓
15	✗	✓	✓	✗	✓	✓	✗	✓	✓
16	✓	✓	✓	✓	✓	✓	✓	✓	✓
17	✓	✓	✓	✓	✓	✓	✓	✓	✓
18	✗	✓	✗	✗	✓	✓	✗	✓	✓
19	✗	✓	✓	✗	✓	✓	✗	✓	✓
20	✓	✓	✓	✓	✓	✓	✓	✓	✓
21	✓	✓	✓	✓	✗	✓	✓	✓	✓
22	✓	✗	✓	✓	✗	✓	✓	✗	✓
23R	✓	✓	✓	✓	✓	✓	✓	✓	✓
23S	✓	✓	✓	✗	✓	✓	✗	✓	✓
24	✓	✓	✓	✓	✓	✓	✓	✓	✓
25	✓	✓	✓	✓	✓	✓	✓	✓	✓
26	✓	✓	✓	✗	✓	✓	✗	✓	✓
27	✓	✗	✓	✓	✗	✓	✓	✗	✓
28	✓	✓	✓	✓	✓	✓	✓	✓	✓
29	✓	✓	✓	✓	✓	✓	✓	✓	✓
30	✓	✓	✓	✓	✓	✓	✓	✓	✓
31	✓	✓	✓	✓	✓	✓	✓	✓	✓
✓	17	18	24	16	17	26	21	22	30
✓	7	7	6	8	12	5	0	4	2
✗	8	7	2	8	3	1	11	6	0

✓ > 95%    ✓ > 50%    ✗ < 50%

**Figure 3.** Overall performance of the DP4+ probabilities computed for compounds 1–31.

of the 31 examples incorrectly assigned but also only two of them were correctly classified in modest probability. In the remaining 29 cases, the right configuration of the epoxide was properly identified in >95% confidence. Comparing the results obtained with uDP4+ and sDP4+ with the corresponding DP4+ values, it is clear that the combination of both scaled and unscaled NMR shifts affords the highest assignment capacity. Interestingly, the performance of uDP4+ (all data) was higher than that found for sDP4+ (all data), indicating that the inclusion of unscaled shifts allows a better differentiation among the candidate structures. This observation emphasizes one of the major differences with the original DP4 formalism which neglects any effect exerted by the unscaled shifts.<sup>8</sup> Another important feature is the error compensation between both scaled and unscaled derived probabilities, meaning that the failure of sDP4+ (for example, compounds 13 and 18) is overcompensated by uDP4+, or vice versa (for example, compound 22), affording good overall results.

A different insightful discussion arises when analyzing the type of data employed for DP4+ analysis, that is, proton and carbon data. Recently, an interesting debate originated about whether one nucleus is more discriminating than the other, and proton has been suggested to allow a better differentiation among stereoisomers.<sup>15</sup> However, in our case, using only <sup>1</sup>H or

<sup>13</sup>C data alone significantly reduced the performance of DP4+ as well as their associated sDP4+ and uDP4+ probabilities. For instance, with the exclusive use of scaled <sup>1</sup>H NMR shifts (sDP4+, H data) or <sup>13</sup>C NMR shifts (sDP4+, C data), eight (26%) or seven isomers (23%), respectively, were incorrectly assigned, whereas seven (23%) were correctly assigned but in modest confidence. However, using both <sup>1</sup>H and <sup>13</sup>C data significantly improved the overall performance (sDP4+, all data), reducing to two (6%) and six (19%) the number of bad and modest examples, respectively. Similar behavior was observed when the series of unscaled chemical shifts (uDP4+) was analyzed. Interestingly, in this case, the results obtained from <sup>13</sup>C NMR data were slightly better than those obtained from <sup>1</sup>H NMR (three vs eight examples incorrectly assigned, respectively, and twelve vs eight examples correctly assigned in modest confidence, respectively), suggesting that when dealing with epoxides, carbon data is the most discriminating one. Nevertheless, the performance of the method significantly improved upon the inclusion of both types of data in the uDP4+ formalism, facilitated by a constructive compensation of errors. This means that a good assignment made by <sup>13</sup>C data often overrides a bad assignment made by <sup>1</sup>H data (for example, compounds 1, 7, 10, 18, 19, 23, and 26) or vice versa (for example, compounds 12 and 27).

This overall compensation of errors is mainly the reason for the nice performance of the DP4+ method. This is particularly relevant when considering that only four examples were perfectly assigned (>95% probability) simultaneously with all the nine DP4+-derived probabilities (compounds 16, 20, 24, and 31), whereas in 19 examples (61% of the total) at least one of the parameters failed by indicating the incorrect isomer in high certainty.

To summarize, our DP4+ strategy yielded excellent results in discerning the relative configuration of spiro or terminal epoxides. In order to obtain high confidence in the assignments, both <sup>1</sup>H and <sup>13</sup>C data must be used, along with scaled and unscaled shifts. To further illustrate the usefulness of this methodology for the organic chemistry community, two case studies of compounds that could not be unequivocally assigned by the exclusive use of experimental NMR are also given and thoroughly analyzed.

**Case Study 1.** As part of our ongoing program aimed at the development of new chiral catalysts from levoglucosenone (32),<sup>16</sup> a biomass-derived bicyclic enone,<sup>17</sup> we envisaged the preparation of 1,2-amino alcohols by aminolysis of the spiro-epoxides 21 and 22, which in turn could be obtained upon epoxidation of the carbonyl group of ketone 33 (Figure 4).

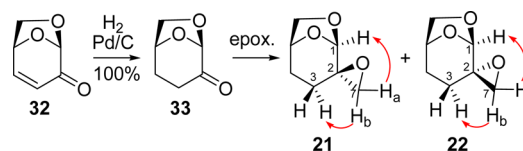


**Figure 4.** Synthesis of spiroepoxides 21 and 22 with key NOE correlations.

Treatment of 33 with diazomethane in chloroform solution afforded two inseparable diastereomeric epoxides 21 and 22 in a 54:46 ratio based on <sup>1</sup>H NMR integration of the mixture. With the intention of providing a pure sample of one isomer, the Corey–Chaykovsky protocol was next employed,<sup>18</sup> and the 21/22 ratio increased to 90:10. All attempts to improve the



selectivity of the reaction met with no success. Nevertheless, we could manage to unequivocally assign all the  $^1\text{H}$  and  $^{13}\text{C}$  resonances of both compounds in the NMR spectra of the mixture by routine combination of 1D and 2D experiments. However, the determination of the absolute configuration at C-2 was ambiguous on the basis of NOE experiments. While irradiation at the H-7a and H-7b signals of the major compound (**21**) afforded an increase at the H-1 and H-3eq signals, respectively, the exact same situation was observed upon irradiation at both H-7 signals of the minor compound (**22**), Figure 4. This observation deserves a further comment regarding the use of NOE for this kind of compounds. The fact that both isomers exhibited the same NOE correlations between the same nuclei raises the question of which assignment would have been made if only one would have been isolated. Probably, in any case, isomer **21** (with the methylene moiety directed toward the  $\alpha$ -face of the molecule, to which are arranged both H-1 and H-3eq) should have been identified as the correct one.

Detailed analysis of the  $^1\text{H}$  NMR spectra of the mixture of **21** and **22** provided further evidence to determine the absolute configuration at C-2. Examination of the signal corresponding to H-7a of the major adduct (**21**) showed long-range coupling ( $J = 1.4$  Hz) with H-3ax (the correlation was also observed from 2D-COSY), indicating a *W* disposition of these two hydrogen atoms. Moreover, such coupling was not observed in the minor isomer (**22**). On the basis of this evidence, we computed the most stable geometries of both adducts at the B3LYP/6-31G\* level of theory (Figure 5). Our calculations

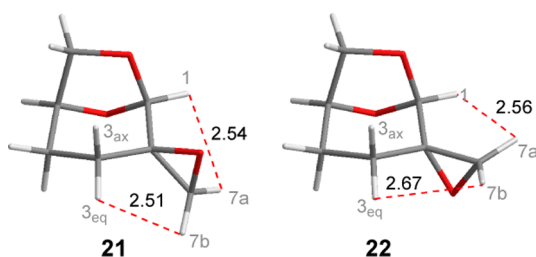


Figure 5. B3LYP/6-31G\*-optimized geometries of compounds **21** and **22** with selected distances (in Å).

showed a clearer *W* relationship between H-7a and H-3ax protons for compound **21**, whereas a more perpendicular arrangement of both hydrogen atoms was observed in the case of **22**. To provide further evidence of this assignment, we next computed the coupling constants of **21** and **22** at the B3LYP/6-31G\* level of theory. The computed  $J_{3\text{ax}-7\text{a}}$  were 1.5 Hz (**21**) and 0.4 Hz (**22**), in excellent agreement with the experimentally found values of 1.4 and  $\sim 0$  Hz, respectively. The other coupling constants were also very well reproduced by our calculations (shown in the SI), increasing our confidence in this computational model. The inconclusive results provided by the NOE experiments can be better understood from the optimized geometries of **21** and **22**, in which no significant differences in the distances between H-7a/H-1 and H-7b/H-3eq computed for both isomers were observed.

The final support of our stereoassignment was made possible by the calculation of the CP3 parameter, introduced by the Goodman group to match two candidates with two sets of experimental data.<sup>7</sup> From the NMR shifts computed at the PCM/B3LYP/6-31+G\*\*//B3LYP/6-31G\* level, the CP3 computed for the matched pairs (major-**21**/minor-**22**) was

0.90 based on both  $^{13}\text{C}$  and  $^1\text{H}$  data, while in the case of the mismatched pairs (major-**22**/minor-**21**), the computed CP3 value was  $-0.98$ , with a very high probability associated with the matched assignment ( $>99.99999\%$ ).

Returning to the original question of what would have happened if only one isomer would have been isolated, Table 1

Table 1. Comparative Results Obtained in the Stereoassignment of **21** and **22** Using DP4 (at the B3LYP/6-31G\*\*//MMFF Level) and DP4+ (at the PCM/mPW1PW91/6-31+G\*\*//B3LYP/6-31G\* Level)

exp NMR from	nuclei	DP4		DP4+	
		21	22	21	22
21	$^1\text{H}$	99.8	0.2	>99.9	<0.1
21	$^{13}\text{C}$	90.0	10.0	99.9	0.1
21	all data	>99.9	<0.1	>99.9	<0.1
22	$^1\text{H}$	99.1	0.9	1.7	98.3
22	$^{13}\text{C}$	87.3	12.7	96.1	3.9
22	all data	>99.9	<0.1	30.1	69.9

shows the DP4+ probability computed for the two isomers using the experimental NMR data of **21** (entries 1–3) and **22** (entries 4–6). We also included the results obtained using the original DP4 formulation to provide insightful comparison between these two methods. Interestingly, only DP4+ succeeded in correctly classifying the two examples under study. On the other hand, DP4 strongly supported isomer **21** in both cases in high confidence, which is actually correct only for the first example. Inclusion of unscaled data and higher level of theory afforded a clear improvement in the overall performance in the stereoassignment of spiroepoxides.

**Case Study 2.** Methionine aminopeptidase 2 (MetAP2) is a metalloprotease involved in the co-translational cleavage of initiator methionines from proteins synthesized in the ribosome. This subtype is up-regulated in several types of cancer, and its selective inhibition allows the suppression of vascularization and growth of tumors.<sup>2d</sup> Therefore, intense research activities have been devoted to the development of MetAP2 inhibitors. In this regard, fumagillin (a metabolite from *Aspergillus fumigatus*) is a potent and selective inhibitor of MetAP2, though it suffers from relatively poor pharmacokinetic profiles.<sup>2d</sup> In an effort to overcome these limitations, Miller and co-workers reported the synthesis and biological evaluation of spiroepoxytriazoles, structurally related to fumagillin.<sup>2b,d</sup> The key and final step of the proposed synthetic scheme involved a DMDO oxidation of the exocyclic alkene present in **34** to afford  $\sim 1:1$  mixtures of the two epimeric epoxides **35** and **36** (Figure 6). According to the authors, the relative configuration of both compounds could not be assigned on the basis of NMR experiments. However, one of the isomers could be crystallized,

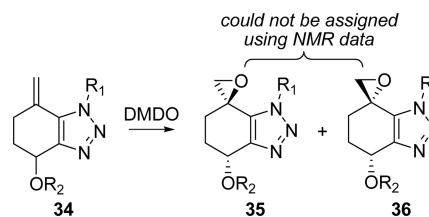


Figure 6. Key and final step for the synthesis of novel MetAP2 inhibitors.

and its structure could be revealed by X-ray analysis. With this pair of compounds with known configuration (compounds **29** and **30**, Figure 2), they subsequently suggested the stereostructure of all other sets of spiroepoxides on the basis of distinctive differences in the  $^1\text{H}$  NMR spectra and  $R_f$  values.

To understand whether the computational methodologies herein discussed could have been useful in this case, we computed the NMR shifts of **29** and **30** at the B3LYP/6-31G\*\*//MMFF and PCM/mPW1PW91/6-31+G\*\*//B3LYP/6-31G\* levels of theory for further DP4 and DP4+ probabilities, respectively (Table 2). Here again, DP4 afforded modest results by indicating **30** as the correct isomer when using the experimental NMR data corresponding to both **29** and **30**, which is only correct in the second case. This inconsistency exhibited by DP4 to strongly support the same isomer regardless of the experimental NMR data employed has been also found by the Fürstner group in their total synthesis and stereochemical revision of mandelalide A.<sup>19</sup> On the other hand, DP4+ nicely identified the correct stereoisomer in high confidence when using the experimental shifts of **29** and **30**, respectively.

**Table 2. Comparative Results Obtained in the Stereoassignment of **29** and **30** Using DP4 (at the B3LYP/6-31G\*\*//MMFF Level) and DP4+ (at the PCM/mPW1PW91/6-31+G\*\*//B3LYP/6-31G\* Level)**

exp NMR from	nuclei	DP4		DP4+	
		29	30	29	30
29	$^1\text{H}$	64.9	35.1	>99.9	<0.1
29	$^{13}\text{C}$	10.0	90.0	88.2	11.8
29	all data	17.0	83.0	>99.9	<0.1
30	$^1\text{H}$	2.2	97.8	<0.1	>99.9
30	$^{13}\text{C}$	1.5	98.5	0.3	99.7
30	all data	<0.1	>99.9	<0.1	>99.9

**Case Study 3.** Since the present study was aimed to evaluate DP4+ in the determination of the relative configuration of terminal or spiroepoxides, we assumed that the remaining stereocenters present in compounds **8–31** (Figure 2) were correctly assigned in the original references. However, in a more realistic scenario, the configuration of more than one stereocenter need to be defined. In order to explore the overall performance of DP4+ in the assignment of organic molecules bearing several stereocenters, we next computed the corresponding probabilities for the full set of diastereoisomers of coriolin and its epimer at the spiroepoxide carbon (compounds **15** and **16**, Figure 2). These compounds represented an interesting case study as they both provide an extra quaternary carbon epoxide unit whose configuration was herein allowed to change. Thus, all 64 possible stereoisomers were generated, and the NMR shielding tensors were computed at the PCM/mPW1PW91/6-31+G\*\*//B3LYP/6-31G\* level on the most significantly populated conformers of each isomer. As indicated in Figure 7, when the experimental NMR data of **15** were used,<sup>20</sup> the DP4+ computed for candidate 4 (the correct structure of **15**) was >99.9%, whereas candidate 36 (the correct structure of **16**) was identified with high confidence when the experimental NMR shifts of **16** were used.<sup>20</sup> Interestingly, in both cases, all of the remaining 63 incorrect structures were assigned in very low overall probability (<0.01%), highlighting

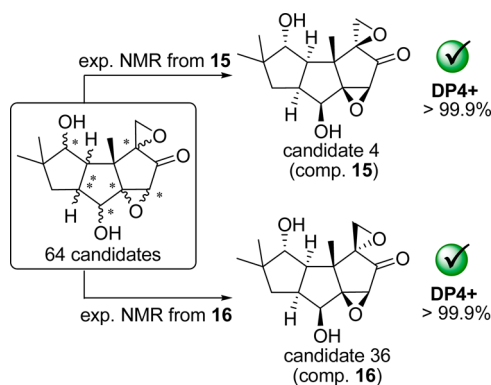


**Figure 7.** Evaluation of DP4+ in the stereoassignment of compounds **15** and **16**. The carbon atoms whose configurations were varied to generate the candidate isomers are marked with an asterisk.

the relevance of our methodology for the stereoassignment of complex organic molecules.

## CONCLUSION

We have tested the performance of our DP4+ probability in several examples of terminal or spiroepoxides bearing a wide variety of molecular complexity and conformational freedom. The excellent levels of correct classification achieved were interpreted on the basis of a constructive compensation of errors observed when using both scaled and unscaled proton and carbon shifts. Therefore, in order to strengthen the confidence in the assignment, both types of data must be used in the DP4+ calculation procedure. Properly used, the DP4+ methodology emerges as a powerful and simple alternative to assign the relative configuration of challenging epoxides from which experimental NMR information affords ambiguous results.

As a final remark, it is important to stress that, as any other computational method used for structural determination purposes, the DP4+ results heavily depend on the quality of the collected experimental and computational NMR data. Incorrectly assigned NMR signals, improper computational work by missing relevant conformers, and/or neglectation of candidate stereostructures might lead to erroneous results. For that reason, those sources or errors should be avoided in order to afford consistent and meaningful predictions.

## EXPERIMENTAL SECTION

**Computational Methods.** All the quantum mechanical calculations were performed using Gaussian 09.<sup>21</sup> In the case of conformationally flexible compounds, the conformational search was done in the gas phase using the MMFF force field (implemented in Spartan 08).<sup>22</sup> All conformers within 5 kcal/mol of the lowest energy conformer were subjected to further reoptimization at the B3LYP/6-31G\* level of theory. The choice for the 5 kcal/mol of cutoff was set as a balance between reducing the overall CPU calculation time and minimizing the possibility of losing further contributing conformers. The conformations within 2 kcal/mol from the B3LYP/6-31G\* global minima were subjected to NMR calculations. The magnetic shielding constants ( $\sigma$ ) were computed using the gauge including atomic orbitals (GIAO) method,<sup>23</sup> the method of choice to solve the gauge origin problem,<sup>5</sup> at the B3LYP/6-31G\*\* (for DP4 calculations) and PCM/mPW1PW91/6-31+G\*\* (for DP4+ calculations) levels of theory. The calculations in solution were carried out using the polarizable continuum model, PCM,<sup>24</sup> with chloroform as the solvent. The unscaled chemical shifts ( $\delta_u$ ) were computed using TMS as the reference standard according to  $\delta_u = \sigma_0 - \sigma_x$ , where  $\sigma_x$  is the

Boltzmann averaged shielding tensor (over all significantly populated conformations) and  $\sigma_0$  is the shielding tensor of TMS computed at the same level of theory employed for  $\sigma_x$ . The Boltzmann averaging was done according to eq 1

$$\sigma^x = \frac{\sum_i \sigma_i^x e^{(-E_i/RT)}}{\sum_i e^{(-E_i/RT)}} \quad (1)$$

where  $\sigma_i^x$  is the shielding constant for nucleus  $x$  in conformer  $i$ ,  $R$  is the molar gas constant ( $8.3145 \text{ J K}^{-1} \text{ mol}^{-1}$ ),  $T$  is the temperature (298 K), and  $E_i$  is the energy of conformer  $i$  (relative to the lowest energy conformer), obtained from the single-point NMR calculation at the corresponding level of theory. The scaled chemical shifts ( $\delta_s$ ) were computed as  $\delta_s = (\delta_u - b)/m$ , where  $m$  and  $b$  are the slope and intercept, respectively, resulting from a linear regression calculation on a plot of  $\delta_u$  against  $\delta_{\text{exp}}$ . The DP4 calculations were carried out using the Applet from the Goodman group (at [www.jmg.ch.cam.ac.uk/tools/nmr/DP4/](http://www.jmg.ch.cam.ac.uk/tools/nmr/DP4/)). The DP4+ calculations were carried out using the Excel spreadsheet available for free at [sarotti-NMR.weebly.com](http://sarotti-NMR.weebly.com), or as part of the Supporting Information of the original paper.<sup>11</sup>

**Experimental Procedures.** All reagents and solvents were used directly as purchased or purified according to standard procedures. Analytical thin-layer chromatography was carried out using commercial silica gel plates, and visualization was effected with short wavelength UV light (254 nm) and a *p*-anisaldehyde solution (2.5 mL of *p*-anisaldehyde + 2.5 mL of  $\text{H}_2\text{SO}_4$  + 0.25 mL of AcOH + 95 mL of EtOH) with subsequent heating. Column chromatography was performed with silica gel 60 H, slurry packed, and run under a low pressure of nitrogen using mixtures of hexane and ethyl acetate. NMR spectra were recorded at 200 or 300 MHz for  $^1\text{H}$  and 50 or 75 MHz for  $^{13}\text{C}$  with  $\text{CDCl}_3$  as solvent and  $(\text{CH}_3)_4\text{Si}$  ( $^1\text{H}$ ) or  $\text{CDCl}_3$  ( $^{13}\text{C}$ , 76.9 ppm) as internal standards. Chemical shifts are reported in delta ( $\delta$ ) units in parts per million (ppm), and splitting patterns are designated as s, singlet; d, doublet; t, triplet; q, quartet; m, multiplet and br, broad. Coupling constants are recorded in hertz (Hz). Isomeric ratios were determined by  $^1\text{H}$  NMR analysis. The structures of the products were determined by a combination of spectroscopic methods such as IR, 1D and 2D NMR (including NOE, DEPT, COSY, HSQC, and HMBC experiments), and HRMS. Infrared spectra were recorded using sodium chloride plates pellets. Absorbance frequencies are recorded in reciprocal centimeters ( $\text{cm}^{-1}$ ). High-resolution mass spectra (HRMS) were obtained on a TOF-Q LC-MS spectrometer.

**Preparation of Spiroepoxides 21 and 22.** Levoglucosenone (32) was obtained from the microwave-assisted pyrolysis of cellulose following our previously reported procedure.<sup>17c</sup> To a solution of 32 (1100 mg, 8.73 mmol) in ethyl acetate (15 mL) was added Pd/C (10%, 110 mg), and the flask was purged by cycles  $\text{H}_2$ /vacuum and stirred under  $\text{H}_2$  atmosphere during 5 h until the total consumption of 32 was determined by TLC. The solution was filtered over Celite and concentrated under reduced pressure to obtain 33 (1100 mg, 8.59 mmol) in 99% yield as a colorless oil, with spectroscopic data identical to those reported by Clark and co-workers.<sup>25</sup> 33:  $[\alpha]_{\text{D}}^{25} = -224.9$  (c 0.635,  $\text{CHCl}_3$ ); IR (film)  $\nu_{\text{max}}$  ( $\text{cm}^{-1}$ ) 2920, 1742(CO), 1111, 986, 883;  $^1\text{H}$  NMR (200 MHz,  $\text{CDCl}_3$ )  $\delta$  5.09 (s, 1 H, H-1), 4.70 (bs, 1 H, H-5), 4.04 (d, 1 H,  $J_{\text{gem}} = 6.0$  Hz, H-6endo), 3.96 (dd, 1 H,  $J_{\text{gem}} = J_{6-5} = 6.0$  Hz, H-6exo), 2.74–1.95 (m, 4 H, H-3 and H-4);  $^{13}\text{C}$  NMR (50 MHz,  $\text{CDCl}_3$ )  $\delta$  200.0 (C, C-2), 101.3 (CH, C-1), 72.9 (CH, C-5), 67.3 ( $\text{CH}_2$ , C-6), 30.9 and 29.7 (2  $\text{CH}_2$ , C-3 and C-4). Finally, epoxides 21 and 22 were prepared from 33 using two different experimental procedures. **Procedure 1.** To a solution of 33 (820 mg, 6.40 mmol) in 15 mL of  $\text{CHCl}_3$  at 0 °C was added a solution of diazomethane in diethyl ether, and stirring continued for 4 h. The excess of diazomethane was quenched after the addition of AcOH, and the solvent was evaporated under reduced pressure. The crude was purified by flash chromatography to give a mixture of epoxides 21 and 22 (496 mg, 3.49 mmol, 55% yield) in a 54:46 ratio determined by integration of the  $^1\text{H}$  NMR spectra of the mixture. **Procedure 2.** NaH (3.96 mmol, 60% dispersion in mineral oil) was placed in round-bottomed flask, and dimethyl sulfoxide (2 mL, distilled from  $\text{CaH}_2$ ) was introduced under argon atmosphere. The resulting mixture was

heated with stirring at 60–70 °C. After 30 min, the reaction mixture was diluted with dry tetrahydrofuran (2 mL) and then cooled to 0 °C. A solution of trimethylsulfonium iodide (2.39 mmol) in saturated dimethyl sulfoxide was added, followed by the addition of a saturated tetrahydrofuran solution of 33 (1.56 mmol) at 0 °C. Stirring was continued for 30 min at 0 °C and then 24 h at room temperature. The reaction was quenched by water (10 mL) and extracted with ethyl acetate (4 × 25 mL). The organic layer was washed with brine (1 × 25 mL), dried ( $\text{Na}_2\text{SO}_4$ ), and concentrated. The residual oil was purified by flash chromatography to afford a mixture of epoxides 21 and 22 (0.91 mmol, 58%) in a 90:10 ratio as a colorless oil: IR (film)  $\nu_{\text{max}}$  ( $\text{cm}^{-1}$ ) 2954, 2897, 1653, 1340, 1292, 1104, 1081, 1021, 988, 970, 899, 885;  $^1\text{H}$  NMR (300 MHz;  $\text{CDCl}_3$ )  $\delta$  4.77 (s, 1H, H-1 of 21), 4.75 (s, 1 H, H-1 of 22), 4.62 (bs, 1 H, H-5 of 21), 4.63 (bs, 1 H, H-5 of 22), 3.98 (d, 2H,  $J_{\text{gem}} = 7.4$  Hz, H-6endo of 21 and 22), 3.84 (m, 2H, H-6exo of 21 and 22), 2.78 (dd, 1 H,  $J_{\text{gem}} = 4.4$  Hz,  $J_{7-3} = 1.4$  Hz, H-7a of 21), 2.75 (d, 1 H,  $J_{\text{gem}} = 4.1$  Hz, H-7a of 22), 2.70 (d, 1 H,  $J_{\text{gem}} = 4.4$  Hz, H-7b of 21), 2.62 (d, 1 H,  $J_{\text{gem}} = 4.1$  Hz, H-7b of 22), 2.31 (m, 1 H, H-3ax of 21), 2.42 (m, 1 H, H-3ax of 22), 2.22 (m, 1 H, H-4 of 22), 2.07 (m, 1 H, H-4 of 21), 1.76 (m, 1 H, H-4 of 21), 1.63 (m, 1 H, H-4 of 22), 1.39 (dddd, 1 H,  $J_{\text{gem}} = 13.4$  Hz,  $J_{3-4} = 5.9$  Hz,  $J_{3-4} = 1.7$  Hz,  $J_{3-5} = 1.4$  Hz, H-3eq of 21), 1.29 (dddd, 1 H,  $J_{\text{gem}} = 14.5$  Hz,  $J_{3-4} = 6.1$  Hz,  $J_{3-4} = 2.7$  Hz,  $J_{3-5} = 1.4$  Hz, 3eq of 22);  $^{13}\text{C}$  NMR (75 MHz;  $\text{CDCl}_3$ )  $\delta$  104.5 (CH, C-1 of 21), 103.9 (CH, C-1 of 22), 73.0 (CH, C-5 of 21), 72.7 (CH, C-5 of 22), 67.7 ( $\text{CH}_2$ , C-6 of 21), 66.9 ( $\text{CH}_2$ , C-6 of 22), 57.8 (C, C-2 of 21), 56.3 (C, C-2 of 22), 52.1 ( $\text{CH}_2$ , C-7 of 21), 50.6 ( $\text{CH}_2$ , C-7 of 22), 28.3 ( $\text{CH}_2$ , C-4 of 21), 26.8 ( $\text{CH}_2$ , C-4 of 22), 23.1 ( $\text{CH}_2$ , C-3 of 21), 23.0 ( $\text{CH}_2$ , C-3 of 22); HRMS-ESI calcd for  $\text{C}_7\text{H}_{11}\text{O}_3$   $[\text{M} + \text{H}]^+$  143.07027, found 143.07018.

## ■ ASSOCIATED CONTENT

### Supporting Information

The Supporting Information is available free of charge on the ACS Publications website at DOI: 10.1021/acs.joc.6b02129.

Full list of the references of the synthesis or isolation of compounds 8–31, full list of experimental chemical shifts, GIAO isotropic shielding tensors, B3LYP/6-31G\* Cartesian coordinates (with energies) and detailed DP4+ probabilities computed for all compounds, and  $^1\text{H}$  and  $^{13}\text{C}$  NMR spectra of compounds 32, 33, 21, and 22 (PDF)

## ■ AUTHOR INFORMATION

### Corresponding Author

\*E-mail: [sarotti@iquir-conicet.gov.ar](mailto:sarotti@iquir-conicet.gov.ar).

### Notes

The authors declare no competing financial interest.

## ■ ACKNOWLEDGMENTS

This research was supported by UNR (BIO 316), ANPCyT (PICT 2011-0255 and PICT-2012-0970), and CONICET (PIP 11220130100660CO). M.M.Z. thanks CONICET for the award of a fellowship.

## ■ REFERENCES

- (1) (a) Yudin, A. K. *Aziridines and epoxides in organic synthesis*; John Wiley & Sons, 2006. For a leading review on epoxides as intermediates in organic synthesis, see: (b) He, J.; Ling, J.; Chiu, P. *Chem. Rev.* **2014**, *114*, 8037. For leading reviews on epoxides in natural products and biologically active compounds, see: (c) Marco-Contelles, J.; Molina, M. T.; Anjum, S. *Chem. Rev.* **2004**, *104*, 2857. (d) Miyashita, K.; Imanishi, T. *Chem. Rev.* **2005**, *105*, 4515. For leading reviews on preparation of chiral epoxides, see: (e) Wong, O. A.; Shi, Y. *Chem. Rev.* **2008**, *108*, 3958. (f) Zhu, Y.; Wang, Q.; Cornwall, R. G.; Shi, Y. *Chem. Rev.* **2014**, *114*, 8199.



- (2) (a) Ekhatov, I. V.; Silverton, J. V.; Robinson, C. H. *J. Org. Chem.* **1988**, *53*, 2180. (b) Miller, A.; Jöst, C.; Klein, C. PCT Pat. Appl. WO2014044399 A1, 2014. (c) Totobenazara, J.; Haroun, H.; Rémond, J.; Adil, K.; Dénès, F.; Lebreton, J.; Gosselin, P. *Org. Biomol. Chem.* **2012**, *10*, 502. (d) Morgen, M.; Jöst, C.; Malz, M.; Janowski, R.; Niessing, D.; Klein, C. D.; Gunkel, N.; Miller, A. K. *ACS Chem. Biol.* **2016**, *11*, 1001. (e) Boratyński, P. J.; Skarzewski, J. *J. Org. Chem.* **2013**, *78*, 4473. (f) Honmura, Y.; Takekawa, H.; Tanaka, K.; Maeda, H.; Nehira, T.; Hehre, W.; Hashimoto, M. *J. Nat. Prod.* **2015**, *78*, 1505. (g) Queiroz, L. H. K.; Lacerda, V.; dos Santos, R. B.; Greco, S. J.; Cunha Neto, A.; de Castro, E. V. R. *Magn. Reson. Chem.* **2011**, *49*, 140.
- (3) (a) Nath, N.; Schmidt, M.; Gil, R. R.; Williamson, R. T.; Martin, G. E.; Navarro-Vazquez, A.; Griesinger, C.; Liu, Y. *J. Am. Chem. Soc.* **2016**, *138*, 9548 and references cited therein. (b) Trigo-Mouriño, P.; Navarro-Vazquez, A.; Ying, J. F.; Gil, R. R. *Angew. Chem., Int. Ed.* **2011**, *50*, 7576 and references cited therein.
- (4) For seminal references, see: (a) Bagno, A.; Rastrelli, F.; Saielli, G. *Chem. - Eur. J.* **2006**, *12*, 5514. (b) Bagno, A.; Rastrelli, F.; Saielli, G. *J. Phys. Chem. A* **2003**, *107*, 9964. (c) Bagno, A. *Chem. - Eur. J.* **2001**, *7*, 1652. (d) Barone, G.; Gomez-Paloma, L.; Duca, D.; Silvestri, A.; Riccio, R.; Bifulco, G. *Chem. - Eur. J.* **2002**, *8*, 3233. (e) Barone, G.; Duca, D.; Silvestri, A.; Gomez-Paloma, L.; Riccio, R.; Bifulco, G. *Chem. - Eur. J.* **2002**, *8*, 3240.
- (5) For leading reviews, see: (a) Grimblat, N.; Sarotti, A. M. *Chem. - Eur. J.* **2016**, *22*, 12246. (b) Lodewyk, M. W.; Siebert, M. R.; Tantillo, D. J. *Chem. Rev.* **2012**, *112*, 1839. (c) Bagno, A.; Saielli, G. *WIREs Comput. Mol. Sci.* **2015**, *5*, 228. (d) Tantillo, D. J. *Nat. Prod. Rep.* **2013**, *30*, 1079. (e) Bifulco, G.; Dambruoso, P.; Gomez-Paloma, L.; Riccio, R. *Chem. Rev.* **2007**, *107*, 3744–3779.
- (6) For leading references, see: (a) Cen-Pacheco, F.; Rodríguez, J.; Norte, M.; Fernández, J. J.; Hernández Daranas, A. *Chem. - Eur. J.* **2013**, *19*, 8525. (b) Lodewyk, M. W.; Soldi, C.; Jones, P. B.; Olmstead, M. M.; Rita, J.; Shaw, J. T.; Tantillo, D. J. *J. Am. Chem. Soc.* **2012**, *134*, 18550. (c) Quasdorf, K. W.; Hutters, A. D.; Lodewyk, M. W.; Tantillo, D. J.; Garg, N. K. *J. Am. Chem. Soc.* **2012**, *134*, 1396. (d) Saielli, G.; Nicolaou, K. C.; Ortiz, A.; Zhang, H.; Bagno, A. *J. Am. Chem. Soc.* **2011**, *133*, 6072. (e) Lodewyk, M. W.; Tantillo, D. J. *J. Nat. Prod.* **2011**, *74*, 1339. (f) Jain, R.; Bally, T.; Rablen, P. R. *J. Org. Chem.* **2009**, *74*, 4017.
- (7) Smith, S. G.; Goodman, J. M. *J. Org. Chem.* **2009**, *74*, 4597.
- (8) Smith, S. G.; Goodman, J. M. *J. Am. Chem. Soc.* **2010**, *132*, 12946.
- (9) (a) Sarotti, A. M. *Org. Biomol. Chem.* **2013**, *11*, 4847. (b) Zanardi, M. M.; Sarotti, A. M. *J. Org. Chem.* **2015**, *80*, 9371.
- (10) (a) Paterson, I.; Dalby, S. M.; Roberts, J. C.; Naylor, G. J.; Guzmán, E. A.; Isbrucker, R.; Pitts, T. P.; Linley, P.; Divlianska, D.; Reed, J. K.; Wright, A. E. *Angew. Chem., Int. Ed.* **2011**, *50*, 3219. (b) Dong, L.-B.; Wu, Y.-N.; Jiang, S.-Z.; Wu, X.-D.; He, J.; Yang, Y.-R.; Zhao, Q.-S. *Org. Lett.* **2014**, *16*, 2700. (c) Novaes, L. F. T.; Sarotti, A. M.; Pilli, R. A. *J. Org. Chem.* **2015**, *80*, 12027.
- (11) Grimblat, N.; Zanardi, M. M.; Sarotti, A. M. *J. Org. Chem.* **2015**, *80*, 12526.
- (12) Chianese, G.; Yu, H. B.; Yang, F.; Sirignano, C.; Luciano, P.; Han, B. N.; Khan, S.; Lin, H. W.; Tagliatela-Scafati, O. *J. Org. Chem.* **2016**, *81*, 5135.
- (13) For the complete list of references of the isolation or synthesis of compounds 8–31, see the [Supporting Information](#).
- (14) In the case of compound **23**, the configuration at the 2' position was not defined by the authors. As a result, herein we considered the two corresponding isomeric pairs, denoted as **23R** and **23S**. That is, in **23R** we compared the two possible configurations at the epoxide center and kept the configuration at C-2' as R. On the other hand, in **23S** we studied the two possible configurations at the epoxide center and kept the configuration at C-2' as S. In both cases, the DP4+ probability correctly assigned the configuration at the epoxide carbon. Moreover, according to the overall DP4+ probabilities, the configuration at C-2' should be R (>99% probability).
- (15) (a) Chini, M. G.; Riccio, R.; Bifulco, G. *Eur. J. Org. Chem.* **2015**, *2015*, 1320. (b) Marell, D. J.; Emond, S. J.; Kulshrestha, A.; Hoyer, T. R. *J. Org. Chem.* **2014**, *79*, 752.
- (16) (a) Gerosa, G. G.; Spanevello, R. A.; Suárez, A. G.; Sarotti, A. M. *J. Org. Chem.* **2015**, *80*, 7626. (b) Sarotti, A. M.; Spanevello, R. A.; Suárez, A. G.; Echeverría, G. A.; Piro, O. E. *Org. Lett.* **2012**, *14*, 2556. (c) Zanardi, M. M.; Botta, M. C.; Suárez, A. G. *Tetrahedron Lett.* **2014**, *55*, 5832. (d) Zanardi, M. M.; Suárez, A. G. *Tetrahedron Lett.* **2015**, *56*, 3762.
- (17) (a) Corne, V.; Botta, M. C.; Giordano, E. D. V.; Giri, G. F.; Llompard, D. F.; Biava, H. D.; Sarotti, A. M.; Mangione, M. I.; Mata, E. G.; Suárez, A. G.; Spanevello, R. A. *Pure Appl. Chem.* **2013**, *85*, 1683. (b) Sarotti, A. M.; Zanardi, M. M.; Spanevello, R. A.; Suárez, A. G. *Curr. Org. Synth.* **2012**, *9*, 439. (c) Sarotti, A. M.; Spanevello, R. A.; Suárez, A. G. *Green Chem.* **2007**, *9*, 1137.
- (18) (a) Peng, Y.; Yang, J.; Li, W. *Tetrahedron* **2006**, *62*, 1209. (b) Corey, E. J.; Chaykovsky, M. J. *Am. Chem. Soc.* **1965**, *87*, 1353.
- (19) Willwacher, J.; Heggen, B.; Wirtz, C.; Thiel, W.; Fürstner, A. *Chem. - Eur. J.* **2015**, *21*, 10416.
- (20) Mizuno, H.; Domon, K.; Masuya, K.; Tanino, K.; Kuwajima, I. *J. Org. Chem.* **1999**, *64*, 2648.
- (21) Frisch, M. J.; Trucks, G. W.; Schlegel, H. B.; Scuseria, G. E.; Robb, M. A.; Cheeseman, J. R.; Scalmani, G.; Barone, V.; Mennucci, B.; Petersson, G. A.; Nakatsuji, H.; Caricato, M.; Li, X.; Hratchian, H. P.; Izmaylov, A. F.; Bloino, J.; Zheng, G.; Sonnenberg, J. L.; Hada, M.; Ehara, M.; Toyota, K.; Fukuda, R.; Hasegawa, J.; Ishida, M.; Nakajima, T.; Honda, Y.; Kitao, O.; Nakai, H.; Vreven, T.; Montgomery, J. A., Jr.; Peralta, J. E.; Ogliaro, F.; Bearpark, M.; Heyd, J. J.; Brothers, E.; Kudin, K. N.; Staroverov, V. N.; Kobayashi, R.; Normand, J.; Raghavachari, K.; Rendell, A.; Burant, J. C.; Iyengar, S. S.; Tomasi, J.; Cossi, M.; Rega, N.; Millam, J. M.; Klene, M.; Knox, J. E.; Cross, J. B.; Bakken, V.; Adamo, C.; Jaramillo, J.; Gomperts, R.; Stratmann, R. E.; Yazyev, O.; Austin, A. J.; Cammi, R.; Pomelli, C.; Ochterski, J. W.; Martin, R. L.; Morokuma, K.; Zakrzewski, V. G.; Voth, G. A.; Salvador, P.; Dannenberg, J. J.; Dapprich, S.; Daniels, A. D.; Farkas, O.; Foresman, J. B.; Ortiz, J. V.; Cioslowski, J.; Fox, D. J. *Gaussian 09*; Gaussian, Inc.: Wallingford, CT, 2009.
- (22) *Spartan'08*; Wavefunction: Irvine, CA.
- (23) (a) Ditchfield, R. *J. Chem. Phys.* **1972**, *56*, 5688. (b) Ditchfield, R. *Mol. Phys.* **1974**, *27*, 789. (c) McMichael Rohlfing, C.; Allen, L. C.; Ditchfield, R. *Chem. Phys.* **1984**, *87*, 9. (d) Wolinski, K.; Hinton, J. F.; Pulay, P. *J. Am. Chem. Soc.* **1990**, *112*, 8251.
- (24) For a review on continuum solvation models, see: Tomasi, J.; Mennucci, B.; Cammi, R. *Chem. Rev.* **2005**, *105*, 2999.
- (25) Sherwood, J.; De Bruyn, M.; Constantinou, A.; Moity, L.; McElroy, C. R.; Farmer, T. J.; Duncan, T.; Raverty, W.; Hunt, A. J.; Clark, J. H. *Chem. Commun.* **2014**, *50*, 9650.